



Incorporation of Silver Nanoparticles with Natural Polymers Using Biotechnological and Gamma Irradiation Processes

M. M. Ghorab¹, A. I. El-Batal², Amro Hanora³ and Farag M. Abo Mosalam^{2*}

¹Department of Pharmaceutical, Faculty of Pharmacy, Suez Canal University, Egypt.

²Department of Drug Radiation Research, Biotechnology Division, National Center for Radiation Research and Technology (NCRRT), Atomic Energy Authority, Egypt.

³Department of Microbiology and Immunology, Faculty of Pharmacy, Suez Canal University, Egypt.

Authors' contributions

This work was carried out in collaboration between all authors. Authors AIEB, MMG and AH wrote the protocol. Authors AIEB, MMG, AH and FMAM designed and analyzed the present study. Authors AIEB, MMG, AH and FMAM wrote the first draft of the manuscript and shared in analysis of the study. Author FMAM managed the literature searches, performed the practical studies and statistical analysis. All authors read and approved the final manuscript.

Article Information

DOI: 10.9734/BBJ/2016/25642

Editor(s):

(1) Miguel Cerqueira, Institute for Biotechnology and Bioengineering, Centre of Biological Engineering, University of Minho, Portugal.

Reviewers:

(1) Carmen Lizette Del Toro Sanchez, Universidad De Sonora, Mexico.

(2) Erwan Rauwel, Tartu College, Tallinn University of Technology, Estonia.

(3) Anonymous, University of Zaragoza, Spain.

(4) Anonymous, Noorul Islam Centre for Higher Education, India.

(5) Satyawati S. Joshi, Savitribai Phule Pune University (Formerly Pune University) Pune, India.

Complete Peer review History: <http://www.sciencedomain.org/review-history/16264>

Original Research Article

Received 13th March 2016
Accepted 25th August 2016
Published 21st September 2016

ABSTRACT

Aim: In this study, silver Nanoparticles (AgNPs) was synthesized by two processes. Chemical process using natural polymers as citrus pectin (CP), chitosan (Cs) and alginate (Alg) and biological process using aqueous extract of fermented fenugreek by *Pleurotus ostreatus* (AEFF).

Methodology: Gamma radiation was used to improve reduction of silver ions to silver nanoparticles (AgNPs) by a chemical process (citrus pectin, chitosan and alginate) and biological process (aqueous extract of fermented fenugreek by *Pleurotus ostreatus*). Optimization of conditions using general factorial design was performed. AgNPs were further characterized by UV-Visible, Dynamic

*Corresponding author: E-mail: farag3m2012@gmail.com;

light scattering (DLS), Transmission Electron Microscopy (TEM), X-Ray diffraction (XRD), Fourier transform infrared spectroscopy (FTIR). Evaluating the anticancer and antioxidant activities of AgNPs was performed.

Results: chemical and biological processes can reduce the silver ions to AgNPs. The maximum AgNPs produced at condition as follows: 1). Chemical process [CP 1%, metal concentration 1 mM, pH 7, radiation dose 5 kGy, size TEM (26 nm), DLS (32 nm) and anticancer IC₅₀ EAC= 35 µg/ml, CACO=39 µg/ml] and 2). Biological process (Aqueous extract of fermented fenugreek powder, metal concentration 0.5 mM, pH 7, radiation dose 20 kGy, size TEM (12.5 nm) DLS (10.3 nm), anticancer IC₅₀ EAC= 2 µg/ml, CACO= 2.4 µg/ml). The incorporation of AgNPs with natural polymer like CP, Cs, Alg and AEFF increases the antioxidant activity.

Conclusion: Synthesis of AgNPs by biological method (AEFF powder by *Pleurotus ostreatus*) it's superior to chemical method (natural polymers as CP, Cs and Alg). AgNPs can be incorporated with natural polymer like CP, Cs, Alg and AEFF; it furthermore, incorporated AgNPs can be used to inhibit the cancer cell and as antioxidant.

Keywords: Natural polymers; gamma radiation; silver nanoparticles; Pleurotus ostreatus; fenugreek; anticancer and antioxidant activities.

1. INTRODUCTION

The synthesis and applications of nanoparticles are gaining intense importance in biomedicine. The size of nanoparticles (1–100 nm), high surface area and reactivity provides them the ability for the therapeutic purpose in different dosage forms and dosing routes. Nanoparticles could be derived from various sources of gas, liquid or solid phases. They can be synthesized using different synthetic methods like physical, chemical, and biological synthesis [1].

AgNPs had been widely used in many applications, such as medical devices, textiles, refrigerators, washing machines and room sprays. The antimicrobial activities of AgNPs had been demonstrated, but the mechanism involved and the cytotoxic effects on human cells have not been fully investigated [2].

Cancer cells survive and multiply due to the decreased intracellular concentration of conventional anticancer drugs. Nanoparticles if properly designed, can cross physiologic barriers due to their small size, delivering drugs in normally inaccessible sites with classical means. Recently, AgNPs has attracted the attention of scientists across the globe for its potent antimicrobial as well as anticancer properties [3].

Green synthesis of AgNPs is considered as one of the cost-effective methods. There are several reports regarding the green synthesis of AgNPs from plant extracts, microbial sources and biopolymers like; chitosan as: Reducing and

stabilizing agents [4]. Bacteria are known to produce inorganic materials either intra- or extracellularly [5].

Polymers such as Cs and Alg can form various chemical bonds with metals' components thus enhancing the stability of the nanoparticles. It has low toxicity therefore, safe for human applications as antimicrobial and anticancer. The reduction can be performed in solutions or as a micro emulsion. In solution, a metal salt is reduced by a certain reducing agent at the present of a stabilizer, that usually a special ligand, polymer, or surfactant [6].

The nano-size droplets are dispersed in incompatible phases like; H₂O-Oil and stabilized by surfactant molecules distributed over the interface. Metal ions in micro emulsion can be reduced to the metal Sol., and the metal particles are naturally protected from aggregation and growth to larger particles [6].

Gamma irradiation was a simple and efficient method for AgNPs synthesis that required an aqueous system, room temperature and ambient pressure[7]. The surface plasmon absorbance (SPA) properties of nanoparticles had a direct relationship to the size, shape, and chemical composition of nanoparticles although intensity and wavelength shift across the SPA absorption spectrum were used to follow growth or particle size [8-9].

Various methods used for colloidal AgNPs synthesis by metal salts, namely chemical reduction, photochemical, electrochemical, microwave processing and irradiation [10].

Irradiation induced reduction synthesis that offers some advantages over the conventional methods like: Its simplicity, it provides metal nanoparticles in fully reduced, greatly pure and considerably stable state [11]. On the other hand biological processes for nanoparticle synthesis had been proposed as feasible eco-friendly alternatives to chemical and physical methods, because they are hazardous and costly [12-13].

In this study, we aim to focus on the synthesis of AgNPs using some nutraceuticals: Chemical process using natural polymers as CP, Cs, Alg and biological process using AEF by *Pleurotus ostreatus*. The anticancer activity and antioxidant activity of synthesized AgNPs were performed.

2. MATERIALS AND METHODS

2.1 Chemicals and Materials

Citrus pectin (CP), silver nitrate (AgNO_3), chitosan (Cs) and sodium alginate (Alg), were obtained from Sigma-Aldrich. Other chemicals and solvents used were of analytical grade.

2.2 Synthesis of Silver Nanoparticle (AgNPs)

2.2.1 Chemical synthesis of silver nanoparticles (AgNPs)

2.2.1.1 By chitosan (Cs) 1%

One gm of Cs was added to 80 ml acetic acid (3%); completed to 100 ml by deionized water. The mixture was stirred at room temperature and placed in dark for overnight. 1 mM AgNO_3 solution was mixed with 1% Cs solution (1:1 v/v.). The mixture was stirred at room temperature and exposed to gamma radiation at (0, 20.0, 40.0, 60.0, 80.0, and 100.0) kGy. This led to the immediate formation of AgNPs that indicated by yellowish-brown color formed. AgNPs were characterized by UV-Visible spectroscopy.

2.2.1.2 By sodium alginate (Alg) 1%

One gm of sodium alginate was added to 100 ml of deionized water. The mixture was stirred at room temperature and placed in dark for overnight. 1mM AgNO_3 solution was mixed with sodium alginate 1% solution (1:1 v/v.). The mixture was stirred at room temperature and exposed to gamma radiation at (0, 10.0, 15.0,

20.0, 25.0, 30.0, 35.0, 40.0, 45.0, and 50.0) kGy. This led to the immediate formation of AgNPs that indicated by yellowish-brown color formed. AgNPs were characterized by UV-Visible spectroscopy.

2.2.1.3 By citrus pectin (CP) 1%

One gm of citrus pectin was added to 100 ml of de ionized water. The mixture was stirred at room temperature and placed in dark for overnight. 1 mM AgNO_3 solution was mixed with citrus pectin 1% solution (1:1 v/v.). The mixture was stirred at room temperature and exposed to gamma radiation at (0, 1.0, 5.0, 15.0, 20.0, and 25.0) kGy. This led to the immediate formation of Ag NPs that indicated by yellowish-brown color formed. AgNPs were immediately characterized by UV-Visible spectroscopy.

2.2.2 Biological synthesis of AgNPs

2.2.2.1 Biological synthesis using fermented fenugreek (seed and powder)

Fungal strain: Locally isolated fungal strain *Pleurotus ostreatus* was used in this study obtained from the culture collection in the Drug Microbiology Laboratory, Drug Radiation Research Department (NCRRT, Egypt). Strain was microscopically identified and kept on potato dextrose agar (PDA) at 4°C and periodically subcultured to maintain viability.

Fermentation medium: Fermentation was carried out in 250 ml Erlenmeyer flasks, distilled water was added to fenugreek seed and powder (60% moisture content) and autoclaved at 121°C for 20 min. The fungus was inoculated to the medium as 2 ml spore suspension (8×10^6 spores/ml) and incubated at 30°C statically in complete darkness for ten days. After that, the whole contents of the flasks were soaked with deionized water (1 g fresh weight / 10 ml) and put in a shaker at 200 rpm (LAB-Line R Orbit Environ, U.S.A) for 2 h. and then centrifuged in cooling centrifuge (Hettich Universal 16 R, Germany) for 10 min at 5°C. The supernatant was separate from sediment and used for experement.

One mM AgNO_3 solution was mixed with aqueous extract of fenugreek (fermented seed or powder) and (unfermented seed or powder) as 1:1 v/v. The mixture was stirred at room temperature and exposed to gamma radiation at (0, 5.0, 10.0, 15.0, 20.0, and 25.0 kGy). This led

to the formation of AgNPs that characterized by UV-Visible.

2.2.2.2 *Biological synthesis using general factorial design*

Used to compare the effect of heat and gamma irradiation on the synthesis of silver nanoparticles by aqueous extract of fermented fenugreek powder (AEFFP). These factors were chosen as they were considered to have the most significant effect on the size of nanoparticles. The levels were selected based on knowledge acquired from initial experimental trials.

2.3 Statistical Analysis

The results of optimization of medium components for optical response were analyzed by using the software version 6.0 (Minitab.11 MP), Also all tests were carried out in duplicate. For comparison and statistical analysis, each of these tests was considered as an individual observation.

Effect of heat: The effects of the three variables in three level form namely: Concentration of silver ions (0.5 mM, 1 mM and 2 mM), pH of reaction mixture (4, 7, and 10) and temperature of reaction mixture (25°C, 60°C and 100°C) were designed.

Effect of gamma radiation: The effects of the two variables in three level form namely: Concentration of silver ions (0.5 mM, 1 mM and 2 mM) and pH of reaction mixture (4, 7, and 10); all samples were exposed to 20 kGy were designed.

The main effects of parameters on silver nanoparticles production were estimated by UV-Visible response optical density (O.D).

2.4 Characterization of AgNPs

Size, morphology and stability of the synthesized AgNPs were characterized using the following techniques.

2.4.1 UV-visible spectral analysis

For the preliminary determination of AgNPs, UV-Visible spectroscopy (T 60 UV/Vis spectrometer) at a resolution of 1 nm was performed to measure the SPR for the wave length ranging from 350-800 nm.

2.4.2 Transmission electron microscopy (TEM)

AgNPs suspension were loaded on carbon-coated copper grids and solvent was allowed to evaporate by incubation at 37°C for 30 min in an incubator. The size and morphology of the AgNPs were estimated by TEM (JEOL electron microscope JEM-100 CX) operating at 80 kV accelerating voltage.

2.4.3 Dynamic light scattering measurement (DLS)

Average particle size and size distribution were determined by the dynamic light scattering (DLS). Technique (PSS-NICOMP 380-ZLS, USA); 250 µl of suspension were transferred to a disposable low volume cuvette. After equilibration to a temperature of 25°C for 2 min., five measurements were performed using 12 runs of 10s each.

2.4.4 Fourier transform infrared spectroscopy (FTIR)

FTIR spectra of the samples were recorded in KBr pellets using an FTIR spectrophotometer (Genesis series, Unicam, England) and spectrum was collected at a resolution of 4 cm⁻¹ in wave number region of 400 to 4000 cm⁻¹ to identify the possible molecules responsible for the reduction of metallic ions and to confirm capped AgNPs.

2.4.5 X-ray diffraction (XRD)

XRD study of AgNPs was done to determine the structural characterization of the nanoparticles by using X-ray diffractometer (Shimadzu XRD 6000 with Cu radiation $\lambda = 1.54056 \text{ \AA}$ at National Center for Radiation Research and Technology (NCRRT), Atomic Energy Authority, Egypt; X ray tube operating at 40 Kv and 30 mA anode current throughout the measurements. In the range of 2 θ value between 0° and 90° with a speed of 8°/min) with preset time 0.15 sec. was used for the 2 θ angle.

2.5 Nitrate Reductase Assay

The prepared aqueous extract of fermented fenugreek powder (AEFFP) was considered for the assay of nitrate reductase according to the method of Harley [14]. Two ml aqueous extract of fermented fenugreek powder was mixed with 2 mL of the assay medium (30 mM KNO₃ and 5% iso-propanol in 0.1 M phosphate buffer of pH 7.5)

and incubated at 25°C in the dark for 1 h and then 1 mL of 50 mM sulphanilamide and 1 ml of 10 mM NEED (N-(1-naphthyl) ethylene diamine dihydrochloride) solutions were added. The intensity of the developed color was estimated in an UV-Vis. spectrophotometer at 540 nm.

2.6 Antioxidant Assay

Antioxidant activity of AgNPs synthesized by both chemical (citrus pectin, alginate and chitosan) and biological process (fermented and unfermented fenugreek powder or seed) was determined by 2,2' diphenyl-1-picryl hydrazyl (DPPH) radical scavenging; the method of Shimada [15] was used to determine the antioxidant activity as 4.0 ml AgNPs was added to methanol solution of 10 mM DPPH (1.0 ml) on individual tubes. The mixture was shaken and left to stand at room temperature for 30 minute. Absorbance of the resulting solution was than measured spectrophotometrically at 517 nm. The inhibitory percentage of DPPH was calculated According to the following equation:

$$\text{Scavenging effect} = [1 - (\text{absorbance sample} / \text{absorbance control})] \times 100\%$$

2.7 Radiation Source

The process of irradiation was carried out at the National Center for Radiation Research and Technology (NCRRT). The facility used was 60-Co Gamma Chamber 4000-A-India. Irradiation was performed using 60 Co- gamma rays at a dose rate 2.21 kGy/h at the time of the experiment. In this process, 60-Co gamma-rays interact with matters in the solution mainly by photoelectric absorption and compton scattering to produce free electrons and also hydrated electrons induced from water radiolysis.

2.8 Anticancer (Cytotoxic Activity)

Ehrlich Ascites Carcinoma Cells (mouse tumor): Ehrlich Ascites Carcinoma Cells (EAC) was kindly supplied by the National Cancer Institute (NCI), Cairo University, Egypt, and was maintained by weekly intraperitoneal transplantation of 2.5×10^6 /ml cells in female Swiss albino mice. A line of Ehrlich Ascites Carcinoma (EAC) cells was supplied from National Cancer Institute, Cancer Biology Department, and maintained by weekly I.P. transplantation of 2.5×10^6 cells / mouse.

2.8.1 Cytotoxicity assay

Assay of cytotoxic activity of AgNPs synthesized by citrus pectin 1%, sodium alginate 1%, chitosan 1% and aqueous extract of fermented fenugreek powder and determine the 50% inhibition of cell survival (IC_{50}) for the best one; under investigation against Ehrlich Ascites Carcinoma cells.

2.8.2 Procedure

Ascites fluid was withdrawn under aseptic conditions (ultraviolet laminar flow system) from the peritoneal cavity of tumor bearing mice by needle aspiration after 7 days of EAC cells inoculation.

Adjust the number of EAC cells/ml, tumor cells obtained was diluted several times with normal saline. EAC viable cells were counted by trypan blue exclusion method where, 10 μ l trypan blue (0.05%) was mixed with 10 μ l of the cell suspensions. Within 5 minutes, the mixture was spread onto haemocytometer, covered with a cover slip and then cells were examined under microscope. Dead cells are blue stained but viable cells are not [16]. Cells suspension was adjusted to contain 2.5×10^6 viable cells/ml.

2.8.3 Trypan blue exclusion method [17]

In sterile test tubes the following were added:

	Tested compound tubes	Control tubes
EAC cells	100 μ l	100 μ l
RPMI medium	800 μ l	900 μ l
Tested compound	100 μ l (of tested compound or and contain different concentrations for IC_{50} estimation)	

Then the cells were incubated for 1 hour at 37°C under a constant over lay of 5% CO_2 .

The EAC viable cells were counted by trypan blue exclusion using haemocytometer as mentioned above.

$$\text{The cell surviving fraction} = (T/C)$$

Where, T and C represent the number of viable cells in a unit volume and C is the number of total (viable + dead) cells in the same unit volume.

IC₅₀ estimation. The IC₅₀ is the concentration of an inhibitor where the response (or binding) is reduced by half. IC₅₀ assay was performed to determine the cytotoxic property of synthesized AgNPs against EAC and CACO cell lines.

A line of Ehrlich Ascites Carcinoma (EAC) cells was supplied from National Cancer Institute, Cancer Biology Department, and maintained by weekly I.P. transplantation of 2.5×10^6 cells / mouse. A line of human colon adenocarcinoma (CACO) cells was obtained from the American Type Culture Collection (ATCC, Rockville, MD). The cells were grown as monolayers in growth on RPMI-1640 medium supplemented with 10% inactivated fetal calf serum and 50 µg/ml gentamycin. The cells were maintained at 37°C in humidified atmosphere with 5% CO₂ and were subcultured two more three times a week.

The cells were grown as monolayers in growth RPMI-1640 medium supplemented with 10% inactivated fetal calf serum and 50 µg/ml gentamycin. The monolayers of 10000 cells adhered at the bottom of the wells in a 96-well microtiter plate incubated for 24 h at 37°C in a humidified atmosphere with 5% CO₂. The monolayers were then washed with sterile phosphate buffer saline (0.01 M pH 7.2) and simultaneously the cells were treated with 100 µl from different dilution of tested sample in fresh maintenance medium and incubated at 37°C. A control of untreated cells was made in the absence of tested sample. Positive control maintaining doxorubicin drug was also tested as reference drug for comparison. Six wells were used for each concentration of the test sample. Every 24 h the observation under the inverted microscope was made. The number of the surviving cells was determined by staining of the cells with crystal violet [18,19] followed by cell lysis using 33% glacial acetic acid and read the absorbance at 590 nm using ELISA reader (sunRise, TECAN, Inc, USA) after well mixing. The absorbance values from untreated cells were considered as 100% proliferation.

The number of viable cells was determined using ELISA reader as previously mentioned before and the percentage of viability was calculated as $[(OD_t/OD_c) \times 100]$ where:

OD_t is the mean optical density of wells treated with the tested sample and OD_c is the mean optical density of untreated sample. 50% inhibitory concentration (IC₅₀); the concentration

required to cause toxic effect in 50% of intact cells, was estimated from graphic plots.

3. RESULTS AND DISCUSSION

3.1 Characterization of AgNPs

3.1.1 UV-visible spectroscopy analysis

3.1.1.1 Chemical synthesized silver nanoparticles (AgNPs)

The change in color (Fig. 1a) and a strong absorption band at 430 nm (Fig. 1b) were indication of AgNPs formation. It is well known that silver nanoparticles exhibit yellowish brown, dark red and greenish color in water; these colors arise due to phenomenon of surface plasmon excitations in the metal nanoparticles [20].

Optical properties of AgNPs were determined by the excitation of plasmon resonances; λ_{max} of AgNPs was found to be 430 nm that confirmed the formation of silver nanoparticles [21]. The peak with very sharp and highest intensity which means there is more yield of silver nanoparticles and size distribution of the silver nanoparticles is narrow [22-24].

Table 1 shows the optical density (O.D) of AgNPs at λ_{max} 430 nm. With unirradiated reduction process, silver nanoparticles were generated with low O.D than irradiated reduction process. The advantage of gamma irradiation process for the synthesis of metallic nanoparticles lies in the fact that desired highly reducing radicals can be generated without formation of any byproduct.

The primary radicals and molecules produced in water upon gamma irradiation are e^-_{aq} , OH^\bullet , H^\bullet , H_2 and H_2O_2 are capable to abstract hydrogen from the polymer producing a polymer radical (secondary radical) [25]. Under the stated experimental conditions the reduction of Ag^+ ions takes place by electron transfer from hydrated electrons and polymer radicals.

We have employed polymers as a reducing agent to Ag^+ ions and a stabilizer for AgNPs. We suggest the following provisional mechanism for gamma irradiation, which is consistent with similar studies on the irradiation reduction of metal nanoparticles (MNPs) in other solutions [22-24] (Eqs. (1) (6).

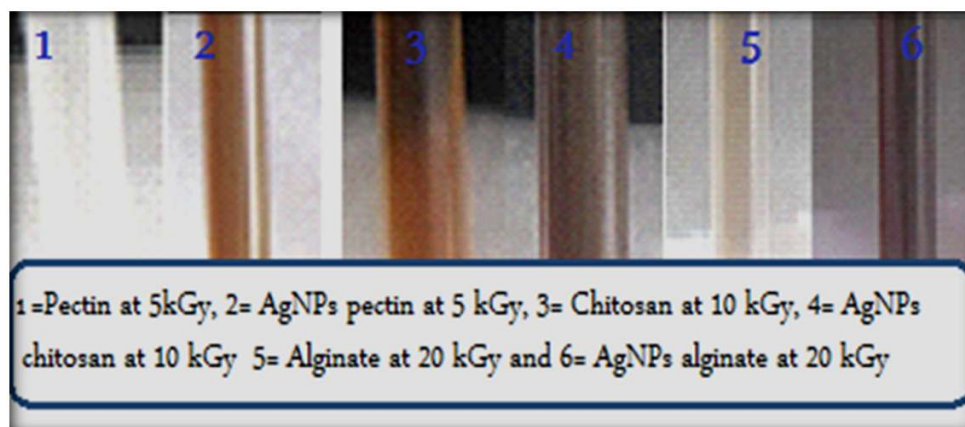
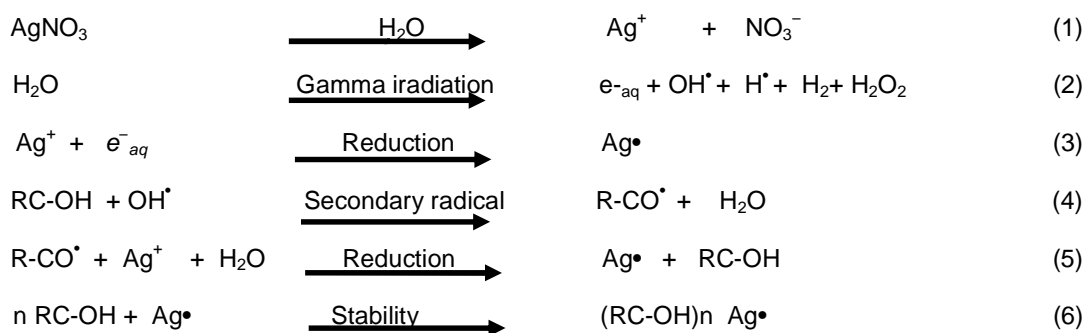


Fig. 1a. Image of silver nanoparticles synthesized by citrus pectin at (5 kGy), chitosan at (10 kGy) and alginate at (20 kGy)

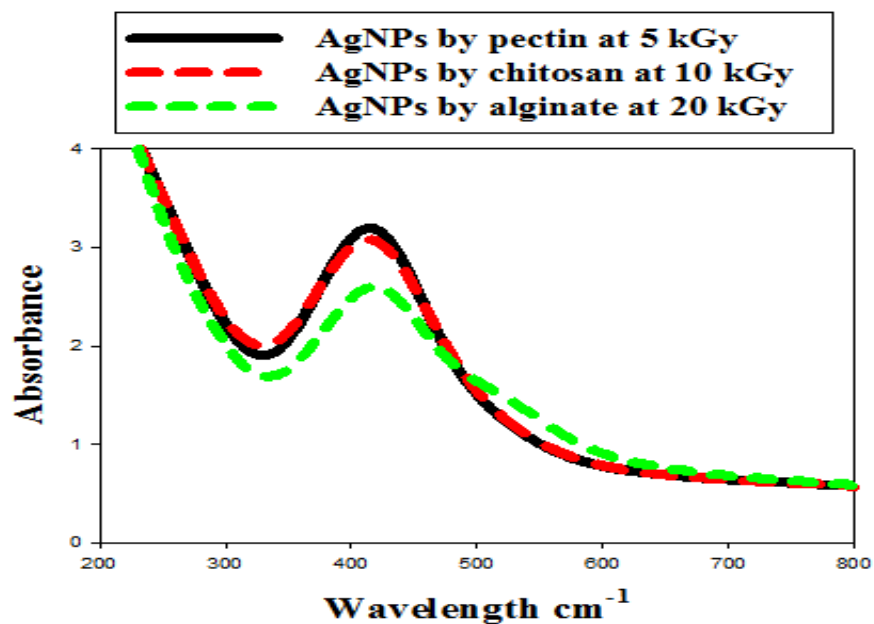


Fig. 1b. UV- visible; silver nanoparticles synthesized by citrus pectin at (5 kGy), chitosan at (10 kGy) and alginate at (20 kGy)

Table 1. Optical density (O.D) of AgNPs synthesized by citrus pectin, chitosan and alginate at different doses of gamma irradiation at λ max 430 nm

Radiation doses (kGy)	AgNPs chitosan; O.D Ab	Radiation doses (kGy)	AgNPs pectin; O.D Ab	Radiation doses (kGy)	AgNPs alginate O.D Ab
0	2.3	0	0.538	0	2.01
10	3	1	1.27	10	2.2
20	2.3	5	3.36	15	2.1
40	2.4	10	2.4	20	2.5
60	2.6	15	2.5	25	1.8
80	2.4	20	2.501	30	2.3
100	2.3	25	1.540	35	2.21
				40	2.22
				45	1.31
				50	1.8

Fig. 1b (best one of polymer O.D) and Table 1 (all polymer O.D) illustrated that, generation of AgNPs depend on types of polymer and dose of radiation; where citrus pectin AgNPs show high optical density (3.36) at 5 kGy, chitosan AgNPs show high optical density (3) at 10 kGy and sodium alginate AgNPs show high optical density (2.5) at 20 kGy.

The optical density O.D of AgNPs synthesized by citrus pectin is higher than chitosan and alginate. This mean that the citrus pectin is superior chitosan and alginate for AgNPs synthesis; may be attributed to formation of degraded unit of citrus pectin that providing the best growth of AgNPs with high stability. Prevent aggregation and agglomeration of metallic nanoparticles. The particle size is probably related to the amount of the stabilizing polymer's chains unites. At a 5 kGy irradiation dose, the amounts of polymer chains increase; the more polymer chains there are, the more they inhibit the aggregation of the silver nanoparticles.

3.1.1.2 UV visible spectroscopy of biological synthesized silver nanoparticles (AgNPs)

The fermentation of fenugreek by *Pleurotus ostreatus* (Fig. 2a) and gamma irradiation play an important role in the synthesis of silver nanoparticles.

After mixing of silver nitrate 1 mM solution with aqueous extract of fenugreek (fermented or unfermented seed and powder) then exposed to gamma irradiation at (0, 5, 10, 15, 20, and 25) kGy.

The appearance of change in color (Fig. 2b) and a strong absorption band at 450 nm (Fig. 2c) is the indication of silver nanoparticles formation.

Fermented fenugreek powder was generated the silver nanoparticles at 20 kGy with high optical density (O.D) and sharp absorption band at range from 400 to 480 nm than other fermented seed, unfermented powder and seed (Fig. 2c O.D of best one). This may be attributed to production of byproducts (amino acid, protein and other fenugreek powder content) that providing the best growth of AgNPs with high stability.

Fig. 2c shows that the fermented fenugreek powder its superior to unfermented powder, fermented and unfermented seed for silver nanoparticles production. This may be attributed to grinding of seed to powder increased the surface area exposed to fermentation. The fermentation process increase the activity and reducing power of fenugreek contents that reduce the silver ions to silver nanoparticles. The 20 kGy is appropriate dose for silver nanoparticles synthesis this may be attributed to production of suitable free electron that reduce silver ions to silver nanoparticles without effect on particles stability.

Gamma irradiation synergism synthesis of silver nanoparticles lies in the fact that desired highly reducing radicals can be generated; the reduction of Ag^+ ions takes place by electron transfer from hydrated electrons (Eqs. (1) (2)).

3.1.2 Experimental factorial design

After carrying out 28 experiments in state of temperature effect and 9 experiments in state of gamma irradiation effect (20 kGy), reflecting different combinations of the variables (Tables 3a and 3b), the results revealed that run number 25 (pH 7, conc.1.0 mM and 25°C) give the highest

AgNPs O.D 1.53 nm (Fig. 3a) than others in state of temperature effect; and run number 9 (pH 7, conc. 1 mM, 25°C and 20 kGy) give the highest AgNPs O.D 7 nm (Fig. 3b) than others in state of gamma irradiation effect.

Figs. 3a and 3b illustrated that, peak area and O.D spectrum obtained from the reaction carried out at pH 7 is considerably higher than those obtained at other pHs (4 and 10) Indicating its higher nanoparticle productivity. This is attributed

to AgNPs tend to precipitation in alkaline pH values which could be due to the formation of silver hydroxide [26,27]. On the other hand acidic pH conditions causes a low negative values of the zeta potential so the silver tend to aggregate and precipitate [28]. The result shows that the synthesis of silver nanoparticles completed at a neutral condition. Acidic or basic pH causes the aggregation of silver nanoparticles to form larger nanoparticles was believed to be favored over the nucleation.



Fig. 2a. Fermentation of fenugreek seed and powder by *Pleurotus ostreatus*

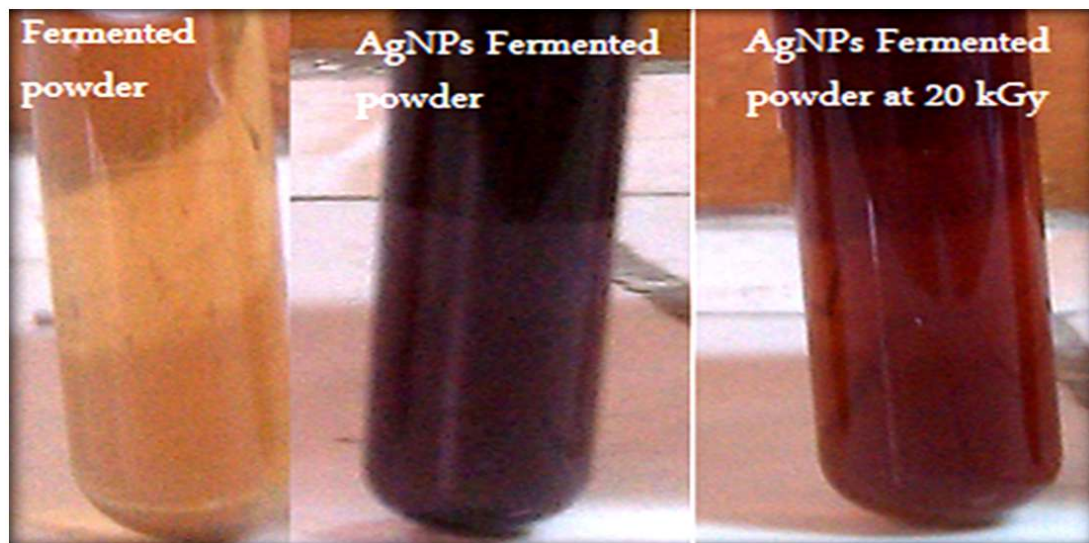


Fig. 2b. Image of silver nanoparticles synthesized by fermented fenugreek using *Pleurotus ostreatus* at 20 kGy

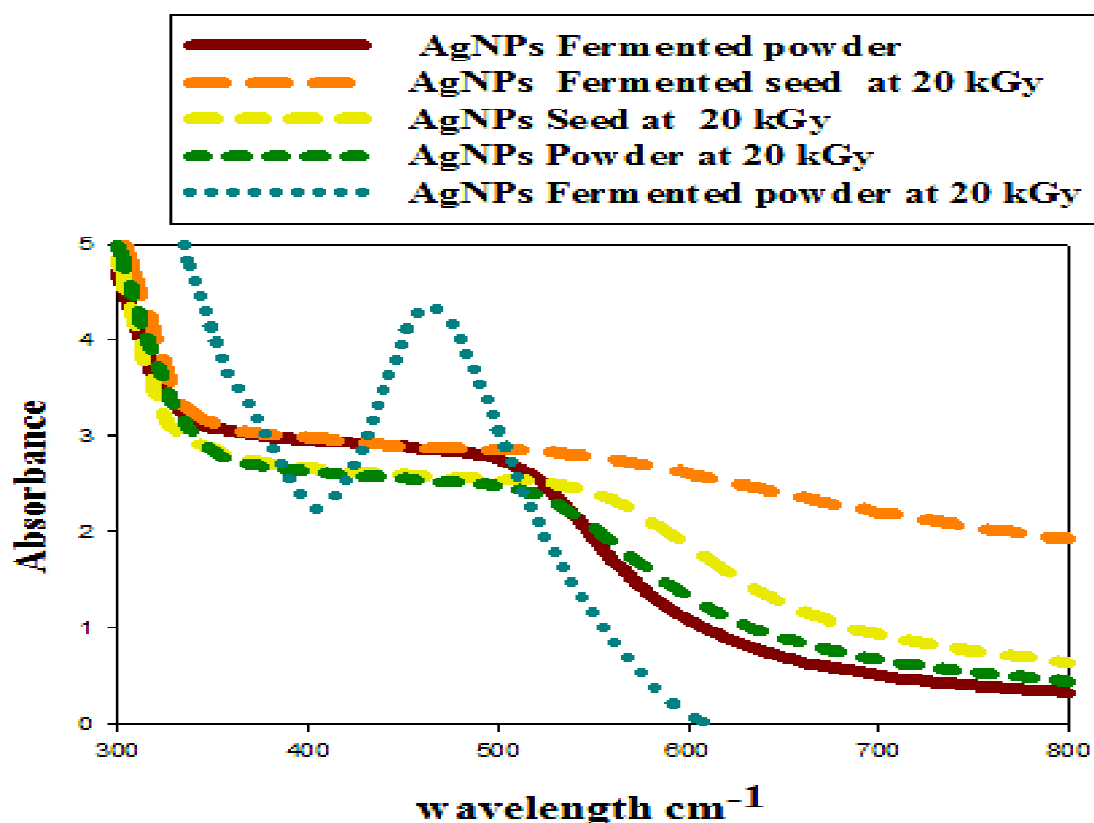


Fig. 2c. UV- visible; silver nanoparticles synthesized by aqueous extract of fenugreek (fermented or unfermented seed and powder) using *Pleurotus ostreatus* at 20 kGy (best one)

The results (Figs. 3a and 3b) clearly indicated that a 1.0 mM concentration of Ag^+ ions was most appropriate for the maximum synthesis of AgNPs. The reason for the decrease optical density with increasing AgNO_3 concentration may also be because AgNO_3 forms a coat on growing particles [29]. The 25°C was most appropriate for the maximum synthesis of AgNPs (Figs. 3a and 3b); this is attributed to Ag^+ ions by increase temperature tend to formation of ion oxide precipitate.

Figs. 3a, 3b and 3c illustrated that gamma irradiation most effective than heat for synthesis of silver nanoparticles, lies in the fact that desired highly reducing radicals can be generated. The reduction of Ag^+ ions takes place by free electrons and secondary radical (Eqs. (1) (6). The slightly broad of the peaks indicates that there is a partially aggregation of particles that redispersed by slightly shaking.

Fig. 3b illustrated that biological synthesis is superior to chemical synthesis for production of silver nanoparticles.

The peak optical density (O.D) of AgNPs synthesized aqueous extract of fermented fenugreek powder (AEFFP) by *Pleurotus ostreatus* (7 nm) its higher than O.D of AgNPs citrus pectin (3.32 nm). This is attributed to presence of byproducts during fermentation (a amino acid, protein, enzymes, fibers,...) that act as reducing agents and stabilizer.

3.1.3 ANOVA for selected factorial model

Statistical analysis of this design demonstrates that the Model F-value of 11.07 implies the model is significant and Values of "Prob > F" less than 0.0500 indicated that model terms are significant. In this case A, B, C are significant model terms.

Values greater than 0.1000 indicate the model terms are not significant.

If there are many insignificant model terms (not counting those required to support hierarchy), model reduction may improve your model.

The "Pred R-Squared" of 0.5782 is in reasonable agreement with the "Adj R-Squared" of 0.6991. "Adeq Precision" measures the signal to noise ratio. A ratio greater than 4 is desirable. The "Adeq Precision" ratio of 11.937 indicates an adequate signal. This model can be used to navigate the design space as mentioned in above Table 3c.

Based on parameter estimates and by applying multiple regression analysis on the experimental data, the response variable and the test variables are related by the following First-order model equation:

Final Equation in Terms of Coded Factors:

$$O.D = +0.62+8.889E-003 * [1] +0.18 * A[2] - 0.15* B[1] +0.30* B[2] 0.21 * C[1] -0.073 * C[2].$$

3.1.4 Transmission electron microscopy (TEM)

TEM images of AgNPs synthesized by citrus pectin at 5.0 kGy and Aqueous extract of fermented fenugreek powder (AFFP) at 20.0 kGy were shown in Figs. 4a and b respectively. The mean size of AgNPs citrus pectin 26 nm and AgNPs aqueous extract of fermented fenugreek powder (AFFP) 12.5 nm.

Figs. 4a and b illustrated that size of AgNPs synthesized by biological process is smallest than that synthesized by chemical process, this is attributed to presence of byproducts during fermentation (amino acid, protein, enzymes, fibers,...) that act as reducing agents and stabilizer prevent aggregation and agglomeration of synthesized AgNPs.

Table 3a. Experimental factorial design experiments response in state of temperature effect

Run	Factor 1 A:pH	Factor 2 B: Conc. mM	Factor 3 C: temp. °C	Response O.D Ab
1	10	0.5	60	0.56
2	7	2	100	0.31
3	10	2	100	0.28
4	4	1	60	0.61
5	10	2	60	0.34
6	10	1	100	0.26
7	7	1	100	1.25
8	7	0.5	25	0.9
9	7	1	60	1.3
10	4	2	25	0.71
11	7	2	60	0.47
12	10	1	25	1
13	10	1	60	0.54
14	4	0.5	60	0.35
15	4	2	60	0.40
16	7	0.5	60	0.38
17	4	1	100	0.57
18	10	0.5	100	0.14
19	10	2	25	0.33
20	10	0.5	25	0.44
21	4	2	100	0.62
22	4	1	25	1.2
23	4	0.5	25	0.67
24	7	2	25	0.8
25	7	1	25	1.43
26	7	0.5	100	0.41
27	4	0.5	100	0.38

Table 3b. Experimental factorial design experiments response in state of gamma radiation effect

Run	Factor 1 A:pH	Factor 2 B:Conc.	Response O.D Ab
1	4	0.5	1.2
2	4	2	1.6
3	10	0.5	1.4
4	10	1	1.8
5	7	1	7
6	4	1	2.8
7	7	0.5	6.5
8	7	2	4.5
9	10	2	1.3

Table 3c. Analysis of variance (ANOVA) for optical density response

Source	Sum of squares	df	Mean square	F value	p-value Prob > F	
Model	2.47	6	0.41	11.07	< 0.0001	Significant
A-pH	0.63	2	0.31	8.45	0.0022	Significant
B-conc.	1.24	2	0.62	16.70	< 0.0001	Significant
C-temp.	0.60	2	0.30	8.06	0.0027	Significant
Residual	0.74	20	0.037			
Cor Total	3.21	26				
Std. dev.	0.19		R-squared		0.7685	
Mean	0.62		Adj R-Squared		0.6991	
C.V. %	30.94		Pred R-Squared		0.5782	
PRESS	1.36		Adeq Precision		11.937	

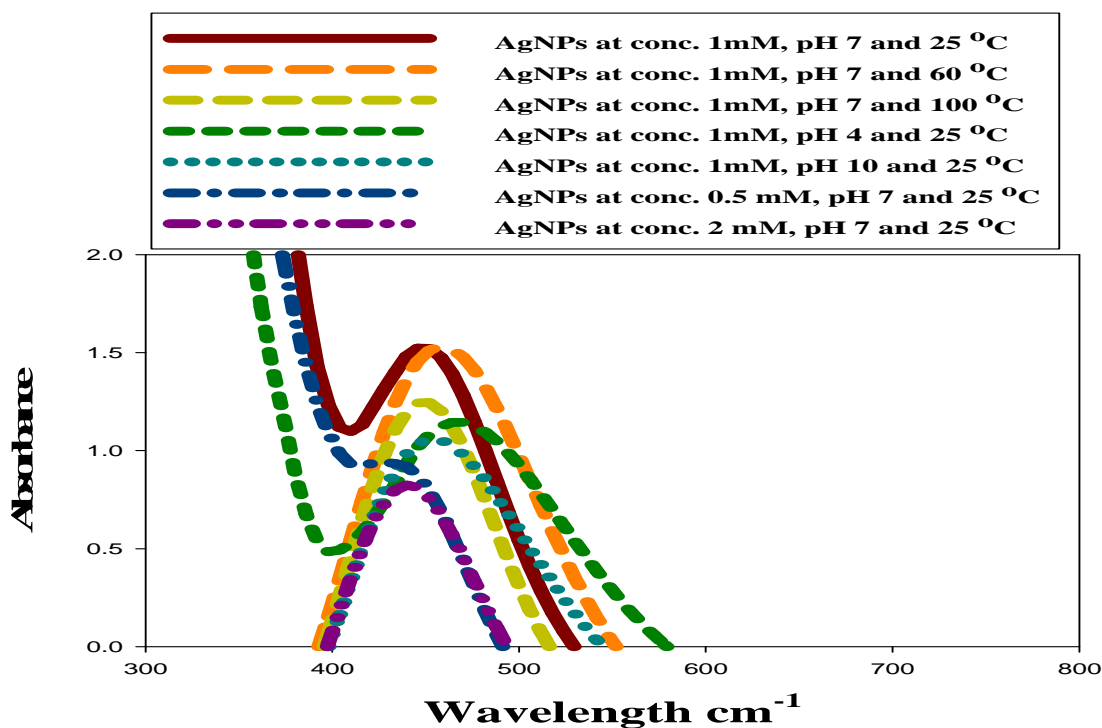


Fig. 3a. UV- visible; silver nanoparticles synthesized using aqueous extract of fermented fenugreek powder by *Pleurotus ostreatus* (highest O.D experimental factorial design experiments) in case of heat effect (best one)

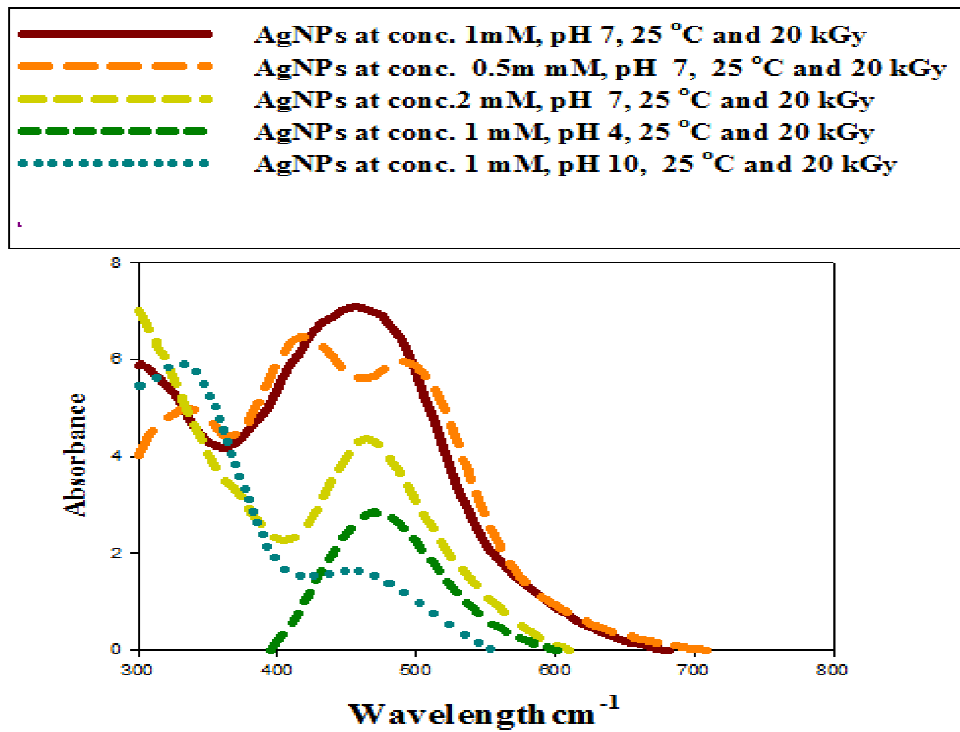


Fig. 3b. UV- visible; Silver nanoparticles synthesized by aqueous extract of fermented fenugreek powder by *Pleurotus ostreatus* (highest O.D experimental factorial design experiments) in case of gamma irradiation effect 20 kGy (best one)

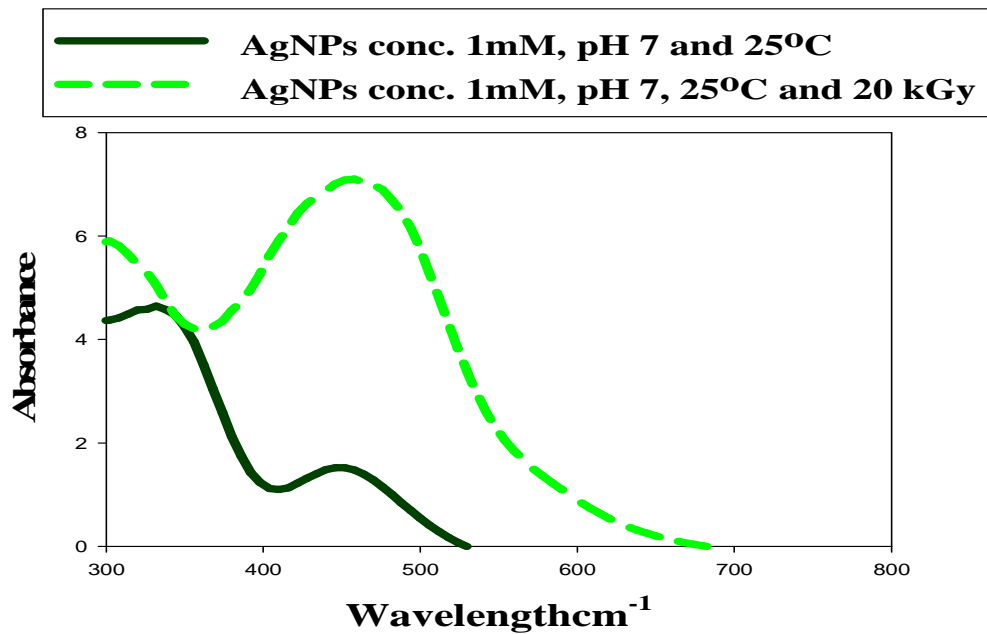


Fig. 3c. UV- visible; silver nanoparticles synthesized by aqueous extract of fermented fenugreek powder by *Pleurotus ostreatus* (highest O.D experimental factorial design experiments) in case of heat and in case of gamma irradiation 20 kGy effect (best one)

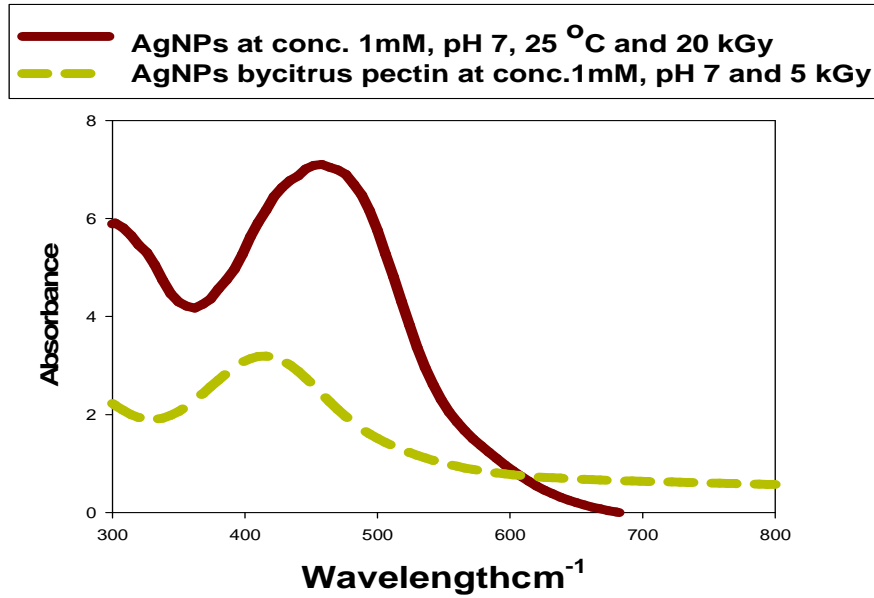


Fig. 3d. UV- visible; compare between AgNPs synthesized by biological (aqueous extract of fermented fenugreek powder by *Pleurotus ostreatus*) and AgNPs synthesized by chemical (citrus pectin) (best one in two process)

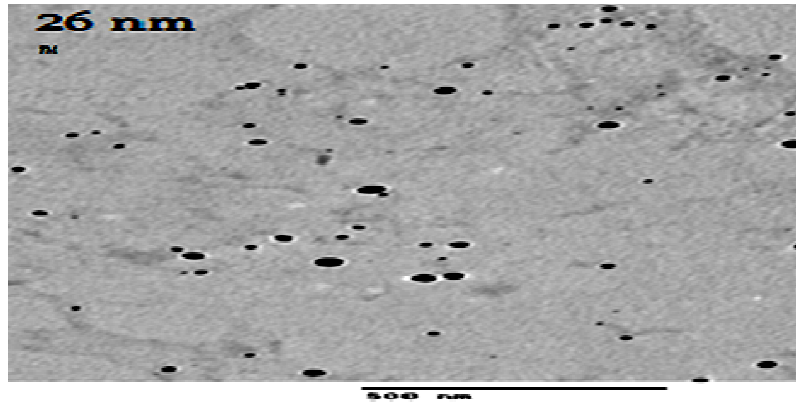


Fig. 4a. TEM Micrograph of AgNPs synthesized by citrus pectin at 5 kGy

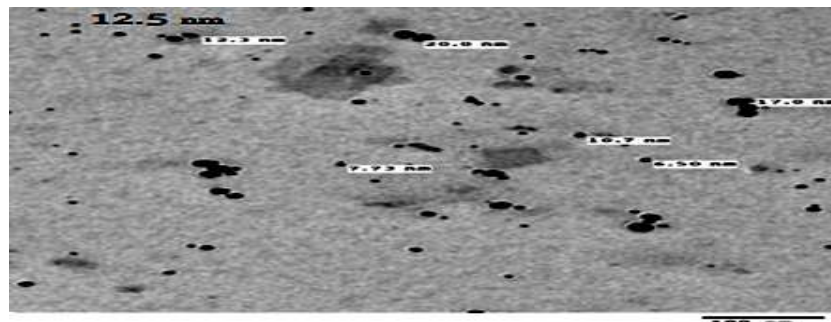


Fig. 4b. TEM Micrograph of AgNPs aqueous extract of fermented fenugreek powder at 20 kGy by *Pleurotus ostreatus*

3.1.5 Dynamic light scattering (DLS)

The particle size distribution of the synthesized AgNPs determined using DLS technique. DLS size range of AgNPs citrus pectin and AgNPs fermented fenugreek powder were found to be 32 nm and 10.3 nm, (Figs. 5a and 5b), respectively. DLS size ranges of AgNPs citrus pectin was found to be greater than TEM size. This might be due to the fact that DLS measures hydrodynamic diameter of nanoparticles, where the amphiphilic nanoparticles were surrounded by water molecules; Moreover, high swelling

properties of pectin in aqueous medium [30] may be attributed to be the cause of large size of capped formulation.

3.1.6 Fourier transform infrared spectroscopy (FTIR)

Figs. 6a and 6b show the FTIR spectra of AgNPs citrus pectin and AgNPs fermented fenugreek powder, respectively. FTIR was carried out to identify the potential biomolecules which is responsible for reduction and capping of the bio-reduced AgNPs.

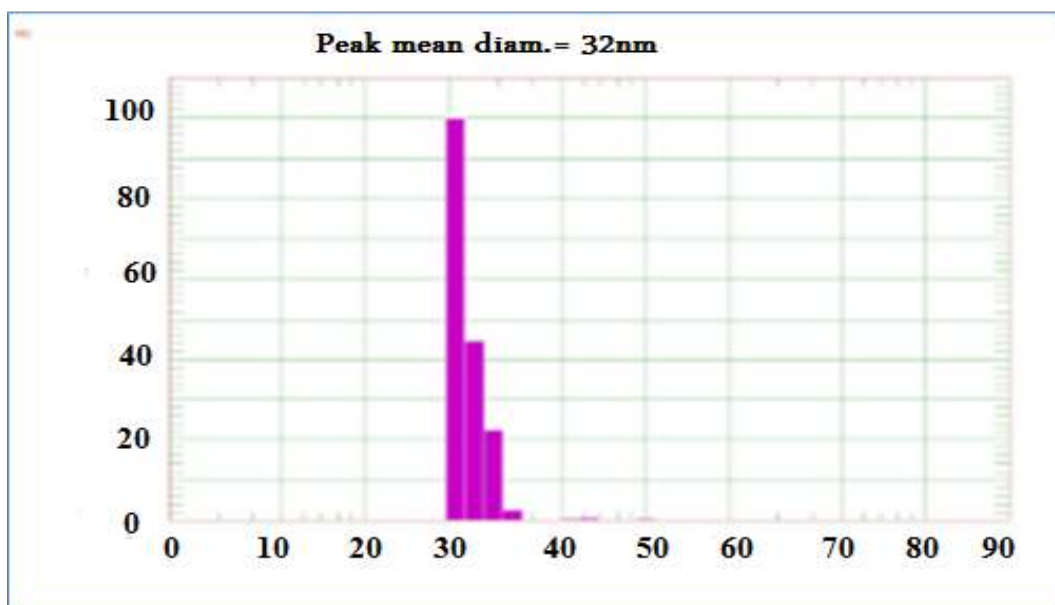


Fig. 5a. DLS graph of AgNPs synthesized by citrus pectin at 5 kGy

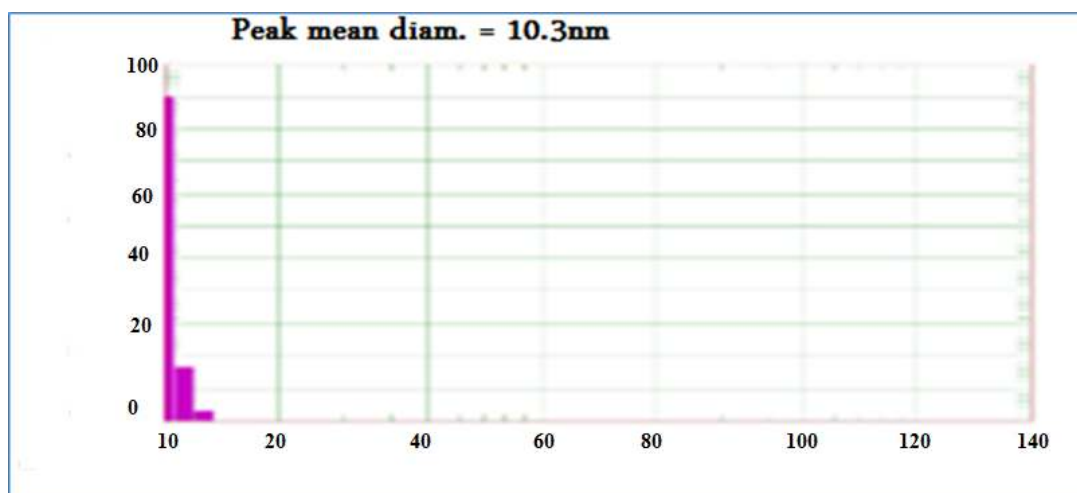


Fig. 5b. DLS graph of AgNPS synthesized by fermented fenugreek powder at 20 kGy by *Pleurotus ostreatus*

Fig. 6a shows; citrus pectin at 0.0 kGy has characteristic absorption bands at 3436 cm^{-1} , 1602 cm^{-1} , 1404 cm^{-1} , 1104 cm^{-1} , 777 cm^{-1} , 1004 cm^{-1} and 740 cm^{-1} . Citrus pectin at 5kGy has absorption bands at 3440 cm^{-1} , 1610 cm^{-1} , 1406 cm^{-1} , 1206 cm^{-1} , 1010 cm^{-1} and 760 cm^{-1} .

AgNPs citrus pectin (AgNPs CP) at 5 kGy has absorption bands at 3442 cm^{-1} , 1612 cm^{-1} , 1409 cm^{-1} , 1210 cm^{-1} , 1015 cm^{-1} and 770 cm^{-1} .

The IR spectrum showed characteristic absorption bands at wave number 3436 cm^{-1} , 3440 cm^{-1} and 3442 cm^{-1} that belongs to OH stretching of pectin. Absorption bands 1602 cm^{-1} , 1610 cm^{-1} and 1612 cm^{-1} indicates carbonyl stretching frequency, 1404 cm^{-1} , 1406 cm^{-1} and 1409 cm^{-1} is that of C-O-H stretching frequency, 1104 cm^{-1} , 1206 cm^{-1} and 1210 cm^{-1} denotes C-C bond stretching frequency, absorption band at 1004 cm^{-1} , 1010 cm^{-1} and 1015 cm^{-1} is that of COOH dimer stretching frequency and bands at 740 cm^{-1} , 760 cm^{-1} and 770 cm^{-1} is associated with carboxylic acid C-OH stretching frequency.

Slightly change of IR spectra with decrease in peak intensity; this mean that AgNPs do not have IR spectra and the spectral peaks that were obtained belonged to the capping agent that indicating OH stretching frequency of the capping agent.

On the other hand, Fig. 6b shows; fermented fenugreek powder at 0 kGy by *Pleurotus ostreatus* had absorption bands at 3370 cm^{-1} ,

2975 cm^{-1} , 1650 cm^{-1} , 1450 cm^{-1} , 1050 cm^{-1} , 777 cm^{-1} , fermented fenugreek powder at 20 kGy by *Pleurotus ostreatus* had absorption bands at 3370 cm^{-1} , 2975 cm^{-1} , 1650 cm^{-1} , 1450 cm^{-1} , 1050 cm^{-1} , 777 cm^{-1} and AgNPs fermented fenugreek powder at 20 kGy by *Pleurotus ostreatus* has absorption bands at 3370 cm^{-1} , 2975 cm^{-1} , 1650 cm^{-1} , 1450 cm^{-1} , 1050 cm^{-1} , 777 cm^{-1} . The broad peak at 3323 cm^{-1} can be assigned to O–H stretching of hydroxyl group and peak at 2975 cm^{-1} corresponds to asymmetric stretching of C–H bonds. The band at 1650 cm^{-1} is assigned to carbonyl and carboxylic (CO) stretching bands of peptide linkages (stretching of amides). The band found at 1450 cm^{-1} can be assigned to –O–H bend of carboxylates. Another band at 1050 cm^{-1} C–N stretching vibrations of primary amines; after the synthesis of silver nanoparticles by fermented fenugreek powder at 20 kGy using *Pleurotus ostreatus* is found to be decrease in the intensity at 3370 cm^{-1} which may be due to binding of Ag⁰ to –OH groups.

The IR spectrum of silver nanoparticles by fermented fenugreek powder has shown the bands (3441, 1590, 1350, 1380, and 757 cm^{-1}) characteristic to proteins suggesting their role in the stabilization of the nanoparticles. It was reported earlier that proteins can bind to nanoparticles either through free amine groups or cysteine residues in the proteins and via the electrostatic attraction of negatively charged carboxylate groups [31] and therefore, stabilization of the silver nanoparticles by proteins is a possibility.

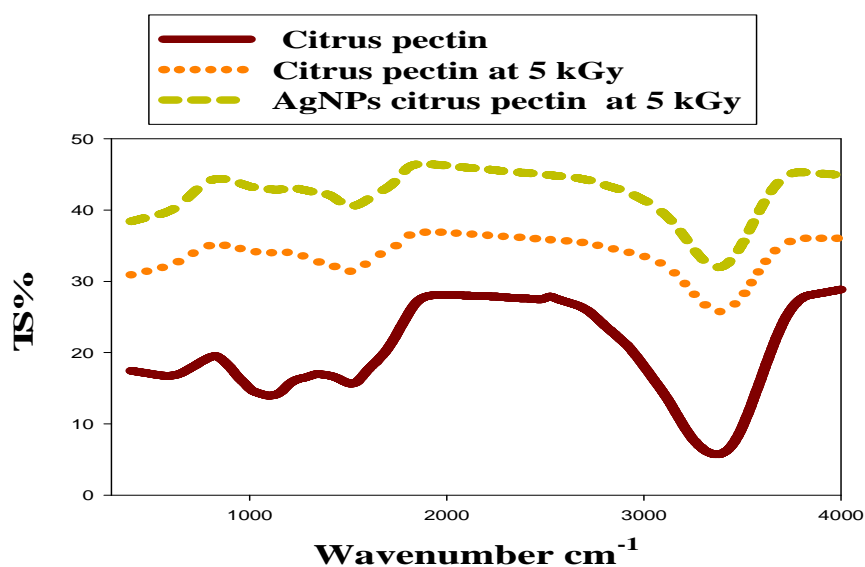


Fig. 6a. FTIR spectra of Ag NPs synthesized by citrus pectin

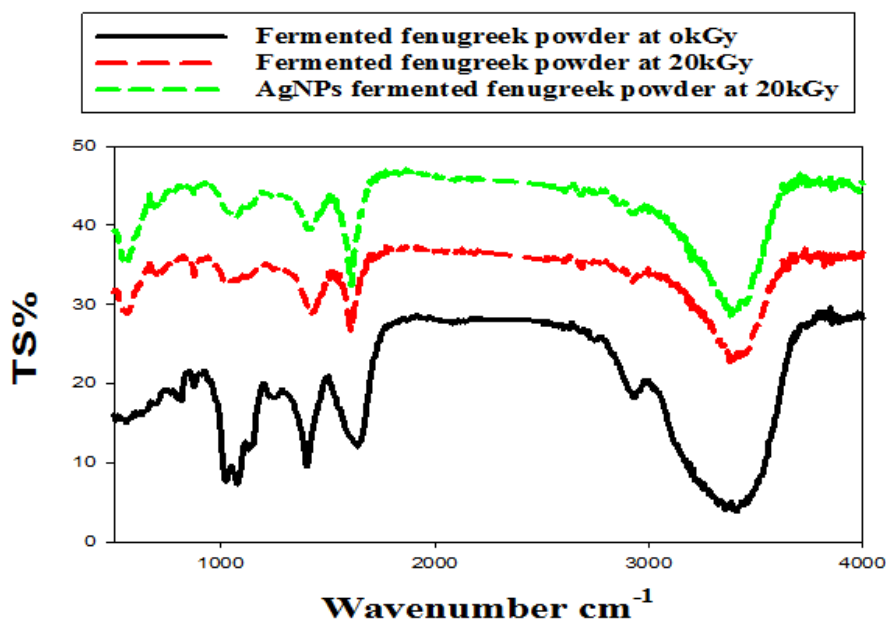


Fig. 6b. Show the FTIR spectra of AgNPs synthesized by aqueous extract of fermented fenugreek powder

3.1.7 X-ray diffraction (XRD)

The crystal structure of AgNPs was further characterized by XRD analysis. The XRD patterns for the synthesized AgNPs by citrus pectin and AgNPs fermented fenugreek powder are reproduced in the Figs. 7a and 7b respectively. The four peaks appear at $2\theta = 37.97^\circ$, 44.11° , 64.35° and 77.27° that corresponds to (111), (200), (220) and (311) planes, respectively, of the face centered cubic AgNPs. The XRD pattern thus clearly shows that the AgNPs formed by the reduction of Ag^+ ions

by citrus pectin and AgNPs fermented fenugreek powder are crystalline in nature.

In addition, residual small peaks are observed at 22.16° in Fig. 7b may be attributed to the peak of protein and amino acid that present in aqueous extract of fenugreek powder.

3.2 Nitrate Reductase Activity

Hence, the role of reductase in the fungus supernatant was investigated by nitrate reductase assay. Nitrate reductase assay was

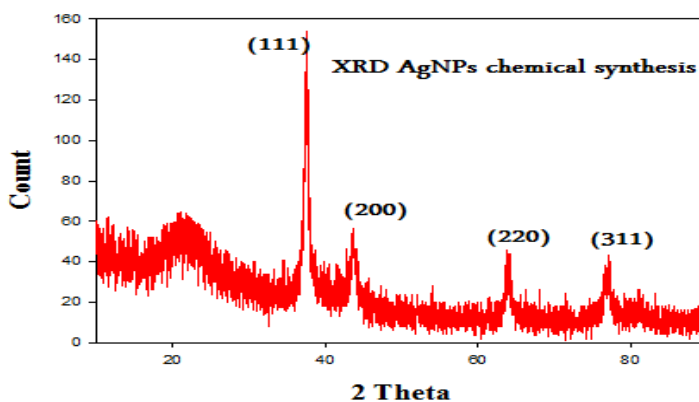


Fig. 7a. XRD pattern for the synthesized AgNPs by citrus pectin at 5 kGy

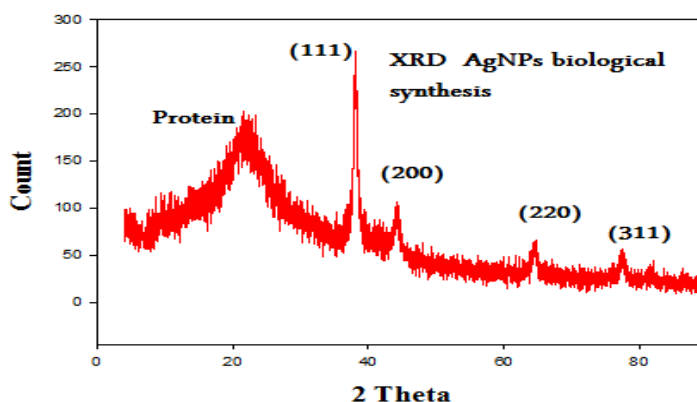


Fig. 7b. XRD pattern for the synthesized AgNPs by fermented fenugreek powder at 20 kGy

investigated in the aqueous extract of fermented fenugreek powder. Our study indicated that *Pleurotus ostreatus* didn't secrete NADH-dependent nitrate reductase enzyme which indicated that other reducing factors may be responsible for the nanoparticles synthesis such as proteins, amino acid and fenugreek powder contents. Silver nanoparticles were stabilized by the proteins and reducing agents secreted by the fungus fermentation of fenugreek powder.

3.3 DPPH Free Radical Scavenging Activity%

Tables 4 and 5 shows the difference in the antioxidant activities after and before AgNPs formation by chemical and biological process respectively.

The antioxidant activities decreased by the increasing of gamma irradiation dose before

silver nanoparticles synthesis; this attributed to antioxidant exhaustion by generated free radical during exposed of aqueous solution to gamma irradiation Equ. (1).

The results also indicated that the marginal increase in antioxidant activity after AgNPs synthesis suggested that the stabilizer and reducer itself is responsible for the majority of the antioxidant activity and AgNPs is not contributing much to the antioxidant activity.

Nanoparticles smaller in size, then having a larger total surface area, were more efficient in the antioxidant activity tests as compared with bigger size stabilizing agents. The antioxidant behavior of these silver phytonanosystems makes them useful in therapy of many diseases caused by oxidative stress [32].

Table 4. Scavenging activity of natural polymer (pectin, alginate and chitosan) and silver nanoparticles using DPPH for assay

Radiation dose (kGy)	Citrus pectin	AgNPs pectin	Radiation dose (kGy)	Chitosan	AgNPs chitosan	Radiation dose (kGy)	Alginate	AgNPs alginate
0	60.32	63.21	0	55.02	60.91	0	50.12	50.41
1	55.43	65.34	10	40.23	45.43	10	60.54	62.52
5	50.61	60.67	20	35.34	40.13	15	55.25	58.83
10	45.48	50.61	40	33.54	35.49	20	45.41	50.46
15	45.89	45.13	60	25.32	28.25	25	40.31	45.76
20	30.13	38.43	80	20.21	25.61	30	30.74	35.38
25	25.52	30.76	100	18.80	20.25	35	30.49	33.21
						40	25.31	28.47
						45	20.32	25.79
						50	20.13	23.94

Table 5. Scavenging activity of unfermented, fermented fenugreek (seed and powder) and AgNPs fermented fenugreek powder using DPPH for assay

Radiation dose (kGy)	Seed	Fermented seed	Powder	Fermented powder	Ag NPs fermented powder
0	35.10	40.35	45.12	50.67	55.23
5	31.43	35.16	41.45	46.89	49.51
10	25.87	31.67	35.21	40.52	45.15
15	21.79	25.81	28.34	36.45	38.62
20	17.12	20.43	25.56	27.90	29.16
25	10.12	15.23	20.12	23.05	25.46

3.4 Anticancer (Cytotoxic Activity)

The preliminary tumor cytotoxic activities of AgNPs synthesized by citrus pectin, sodium alginate, chitosan and aqueous extract of fermented fenugreek powder were evaluated against EAC cells at 1 concentrations using trypan blue 0.5% assay.

Table 6 summarize the cytotoxicity data of citrus pectin, sodium alginate, chitosan and aqueous extract of fermented fenugreek powder alone and after silver nanoparticles synthesis against EAC cells after 1 hour of incubation.

The data were expressed as surviving percent. The results showed that EAC cells proliferation was significantly inhibited by AgNPs synthesized by citrus pectin and fermented fenugreek powder at 5 kGy and 20 kGy respectively than others.

IC₅₀ assay was performed to determine the cytotoxic property of AgNPs synthesized by citrus pectin and fermented fenugreek powder at 5 kGy and 20 kGy respectively against EAC and CACO cell lines.

Treatment of cancer cells with AgNPs at increasing concentrations (0.78 - 50 µg/ml; Tables 7a and 7b) showed cytotoxicity against EAC with 50% inhibition of cell survival (IC₅₀) at concentration of 2 µg/ml (Fig. 8a) and 35 µg/ml (Fig. 8b) for fermented fenugreek powder at 20 kGy and citrus pectin at 5 kGy respectively.

The *in vitro* cytotoxicity of the AgNPs was evaluated against CACO cell line at different concentrations (1.56 - 50 µg/ml; Tables 8a and b); the result showed that CACO cells proliferation was significantly inhibited by AgNPs with the IC₅₀ value 2.4 µg/ml (Fig. 9a) and 39.5 µg/ml (Fig. 9b) for fermented fenugreek powder at 20 kGy and citrus pectin 5 kGy respectively.

In vitro cytotoxicity tests of the AgNPs synthesized by citrus pectin and AgNPs

fermented fenugreek it was observed that fermented fenugreek AgNPs more effective than AgNPs citrus pectin; this strongly indicated that incorporation of AgNPs modified the chemical nature of the AgNPs and cause change the interaction with other molecules such as proteins and others.

Silver nanoparticles synthesized by biological process its more effective as anticancer agents than which synthesized by chemical; this may be attributed to metals are free movement and it can be given effect other than in case of chemical method it capped vigorously and difficult movement which reduces the effect. Also the size play important role in acting as anticancer. The smallest size nanoparticles had the ability to penetrate the cancer cell faster than largest nanoparticles this is clearly shown when comparing AgNPs synthesized by chemical (large size) with AgNPs biological process (the smallest size).

The silver nanoparticles of 26 nm and 12.5 nm are coated with citrus pectin (AgNPs CP) and aqueous extract of fermented fenugreek powder (AgNPs AEFPP) respectively, taken with a series of increasing concentrations (0.78, 1.56, 3.125, 6.25, 12.5, 25 and 50 µg/ml). The AgNPs FFP show high cytotoxicity effect compared to AgNPs CP. This is mainly due to the fact that fermented fenugreek powder has cytotoxic effect more than citrus pectin so as synergistic. More over the particle sizes are difference in AgNPs FFP (26 nm) than AgNPs CP (12.5 nm).

Comparison of the reducing and stabilizing agents revealed that citrus pectin and fermented fenugreek produced more pronounced response and sensitivity to the Cytotoxicity. The cell viability results indicate that silver nanoparticles are toxic to the EAC and CACO cells. The incorporation of surface functionalities via citrus pectin and fermented fenugreek renders these nanoparticles highly biocompatible.

In this study, it was observed that the synthesized AgNPs induces a concentration dependent inhibition of EAC and CACO cells. Cytotoxic effects of silver nanoparticles was probably due to the fact that AgNPs may interfere with the proper functioning of cellular proteins and induce subsequent changes in cellular chemistry provide a relatively high hydrophobicity inside bovine hemoglobin which causes a transition from alpha helixes to beta sheets and leads to partial unfolding and aggregation of the protein [33]. Other reports suggest that AgNPs are likely to interact with thiol rich enzymes. Therefore, it is possible that once penetrated into cells, AgNPs may attack functional proteins of cells which results in partial unfolding and aggregation of proteins [34].

Hence in this study the size dependent cytotoxicity and stabilizing agents are responsible for cytotoxicity. These results are consistent with previous investigations [32] which demonstrated that the stabilizing agents has role for cytotoxicity.

Fenugreek extract has a very selective cytotoxicity against cancer cell lines such as T-cell lymphoma (TCP), B-cell lymphomas, Thyroid Papillary carcinoma (FRO) and breast cancer (MCF7). On the other hand, there was no significant cell cytotoxicity amongst normal cells, including human lymphocytes and meningioma, when treated with fenugreek [35]. This clearly indicates that fenugreek has selective cytotoxic effects against cancer cells. Pectin seems to exert antitumor activity on different cell lines and these probably through different effects. These mechanisms depend on the structure of pectin or on the modified form of pectin that is likely to yield to various active fragments [36].

Silver nanoparticles have proven cytotoxic effects against HeLa cells and MCF-7 cells. Natural products have shown great promise in mitigating carcinogenesis and associated cellular aberrations, with substantial numbers of anticancer agents being derived from natural sources, pectin is a natural plant polysaccharide with mounting reports documenting its anti-tumour efficacy [37]. Due to the limited bioavailability and nondegradable nature of plant pectin, scientists have developed modified citrus pectin (MCP) and fractionated pectin powder (FPP) with better anticancer efficacy.

Fractionated pectin powder was reported to induce significant apoptotic activity than its counterpart MCP with its antitumour activities being mediated by the inhibition of Gal-3 and Gal-3 mediated interactions [38].

Silver nanoparticles inhibit vascular endothelial growth factor (VEGF) induced angiogenesis in bovine retinal endothelial cells. The potent antiangiogenic and antipermeability effects of AgNPs, along with their ability to halt tumor progression in P155 lymphosarcoma cells, have prompted the study of the antitumor effect of AgNPs in ascitic tumors [39]. Silver nanoparticles may be employed as an effective treatment agent against various types of cancers [40].

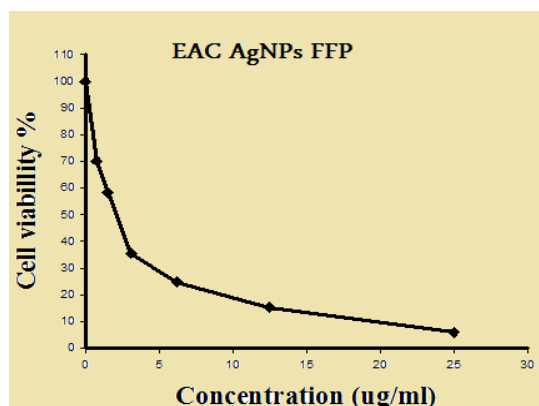


Fig. 8a. Cytotoxicity of Ag NPs fermented fenugreek powder (Ag NPs FFP) against (EAC) cells; IC₅₀ (2 µg/ml)

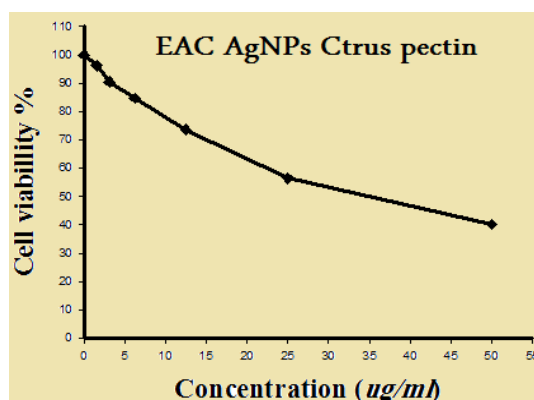


Fig. 8b. Cytotoxicity of AgNPs citrus pectin at 5 kGy (AgNPs CP) against (EAC) cells IC₅₀ (35 µg/ml)

Table 6. Survival cell % in Ehrlich ascites carcinoma cell as affected by AgNPs synthesized by citrus pectin, sodium alginate, chitosan and fermented fenugreek powder using gamma radiation

Radiation dose (kGy)	CP	AgNPs CP	Radiation dose (kGy)	Cs	AgNPs Cs	Radiation dose (kGy)	Ale	AgNPs Alg	Dose of radiation kGy	AEFF P	AgNPs AEFFP
0	90.01	50.22	0	90.31	70.15	0	100	100	0	10.01	10.14
1	55.23	45.34	10	85.12	65.14	10	100	100	1	10.13	8.46
5	50.49	40.41	20	80.70	65.67	15	100	100	5	12.62	10.91
10	65.14	42.57	40	95.09	50.91	20	100	100	10	15.34	14.21
15	68.03	50.12	60	95.76	85.26	25	100	100	15	17.76	15.46
20	70.43	60.78	80	100.0	90.41	30	100	100	20	20.03	6.72
25	80.32	80.51	100	100.0	90.79	35	100	100	25	21.32	10.52
						40	100	100			
						45	100	100			
						50	100	100			

CP = Citrus pectin, Cs = Chitosan, Alg = Alginate and AEFFP = Aqueous extract of fermented fenugreek powder

Table 7a. Surviving percent in (EAC) cells as affected by different concentrations of Ag NPs fermented fenugreek powder at 20 kGy (AgNPs FFP) after 1 hour incubation

Sample conc. (µg/ml)	Viability %
25	6
12.5	15.22
6.25	24.8
3.125	35.55
1.56	58.24
0.78	70.16
0	100.00

Table 7b. Surviving percent in (EAC) cells as affected by different concentrations of AgNPs citrus pectin at 5 kGy (AgNPs CP) after 1 hour incubation

Sample conc. (µg/ml)	Viability %
50	40.16
25	56.43
12.5	73.54
6.25	84.71
3.125	90.43
1.56	96.22
0	100.00

Table 8a. Surviving percent in (EAC) cells as affected by different concentrations of AgNPs fermented fenugreek powder at 20 kGy (Ag NPs FFP) after 1 hour incubation

Sample conc. (µG/ml)	Viability %
25	8.79
12.5	17.24
6.25	28.71
3.125	39.85
1.56	61.84
0.78	73.26
0	100.00

Table 8b. Surviving percent in (CACO) cells as affected by different concentrations of AgNPs citrus pectin at 5 kGy (AgNPs CP) after 1 hour incubation

Sample conc. (µg/ml)	Viability %
50	42.36
25	60.53
12.5	78.24
6.25	89.61
3.125	94.53
1.56	98.72
0	100.00

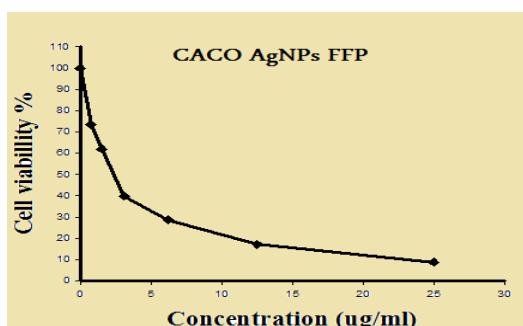


Fig. 9a. Cytotoxicity of Ag NPs fermented fenugreek powder (Ag NPs FFP) against (EAC) cells; IC₅₀ (2.4 µg /ml)

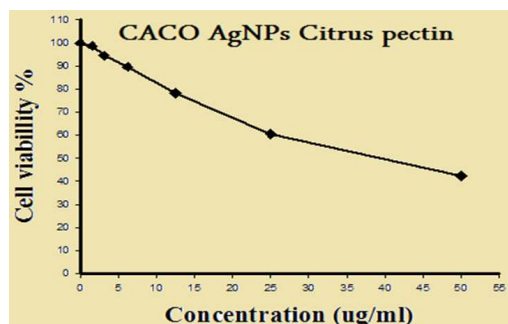


Fig. 9b. Cytotoxicity of AgNPs citrus pectin at 5kGy (AgNPs CP) against (CACO) cells IC₅₀ (39.5 µg /ml)

4. CONCLUSION

Aqueous extract of fermented fenugreek by *Pleurotus ostreatus* can reduce silver ions to AgNPs superior than natural polymers and gamma irradiation improve its synthesis. AgNPs can be incorporated with natural polymer as citrus pectin, alginate, chitosan and fermented fenugreek powder and inhibit the cancer cell with potent effect on EAC than CACO. Synthesized AgNPs have potential effect as antioxidant.

ACKNOWLEDGEMENTS

The authors would like to thank the Nanotechnology Research Unit (P.I. Prof. Dr. Ahmed El-Batal), Drug Radiation Research Department, National Center for Radiation Research and Technology (NCRRT), Egypt, for financing and supporting this study under the project " Nutraceuticals and Functional Foods Production by using Nano/Biotechnological and Irradiation Processes.

COMPETING INTERESTS

Authors have declared that no competing interests exist

REFERENCES

1. Iravani S, Korbekandi HS, Mirmohammadi V, Zolfaghari B. Synthesis of silver nanoparticles: Chemical, physical and biological methods. *Res. Pharm. Sci.* 2015; 9(6):385–406.
2. Banalaa RR, Nagatib VB, Karnati PR. Green synthesis and characterization of Carica papaya leaf extract coated silver nanoparticles through X-ray diffraction, electron microscopy and evaluation of bactericidal properties. *Saudi Journal of Biological Sciences.* 2015;22(5):637–644.
3. Moharana K, Zabeau L, Peelman F, Ringler P, Stahlberg H, Tavernier J, Savvides SN. Structural and mechanistic paradigm of leptin receptor activation revealed by complexes with wild-type and antagonist leptin. *Structure.* 2014;22:866–877.
4. Venkatesham M, Ayodhya D, Madhusudhan A, Veera N, Veerabhadram G. A novel green one-step synthesis of silver nanoparticles using chitosan: Catalytic activity and antimicrobial studies. *Applied Nanoscience.* 2013;4:113–119.
5. Rauwel P, Kuunal S, Ferdov S, Rauwel E. A review on the green synthesis of silver nanoparticles and their morphologies studied via TEM. *Advances in Materials Science and Engineering.* 2015;682749:9.
6. Adliom A. Preparations and application of metal nanoparticles. *Indonesian Journal of Chemistry.* 2006;6(1):1-10.
7. Li J, Kang B, Chang S, Dai Y. Gamma radiation synthesis of plasmonic nanoparticles for dark field cell imaging. *Radiation Physics and Chemistry.* 2012; 76:290–1194.
8. El-Batal AI, Mohamed HE, Bahgat MR, Ahmed AZA. Marine streptomyces cyaneus strain alex-SK121 mediated eco-friendly synthesis of silver nanoparticles using gamma radiation. *British Journal of Pharmaceutical Research.* 2014;4(21): 2525-2547.
9. Naghavi K, Saion E, Rezaee K, Yunus WM. Influence of dose on particle size of colloidal silver nanoparticles synthesized by gamma radiation. *Radiation Physics and Chemistry.* 2010;79:1203–1208.
10. Ramnani SP, Biswal J, Sabharwal S. Synthesis of silver nanoparticles supported on silica aerogel using gamma radiolysis. *Radiation Physics and Chemistry.* 2006; 76:1290–1294.
11. El-Batal AI, Mona S Al Tamie. Optimization of melanin production by *Aspergillus oryzae* and incorporation into silver nanoparticles. *Der Pharmacia Lettre.* 2016; 8(2):315-333.
12. Sinha S, Pan L, Chanda P, Sen KS. Nanoparticles fabrication using ambient biological resources. *Journal of Applied Science.* 2009;19:1113-1130.
13. El-Batal AI, Nora M. ElKenawy, Aymen S. Yassin, Magdy A. Amin. Laccase production by *Pleurotus ostreatus* and its application in synthesis of gold nanoparticles. *Biotechnology Reports.* 2015;5:31–39.
14. Prathna TC, Raichur AM, Chandrasekaran N, Mukherjee A. Biomimetic synthesis of silver nanoparticles by *Citrus limon* (lemon) aqueous extract and theoretical prediction of particle size. *Colloids Surf B Biointerfaces.* 2011;82:152–159.
15. Mukherjee P, Senapati S, Mandal D, Ahmad AM, Khan I, Kumar R, Sastry M. Extracellular synthesis of gold nanoparticles by the fungus *Fusarium oxysporum*. *Chem Bio Chem.* 2002;461-463.
16. Shimada K, Fujikawa K, Yahara K, Nakamura T. Antioxidative properties of xanthan on the anti-oxidation of soybean oil in cyclodextrin emulsion. *J. Agric. Food Chem.* 1992;40:945–948.
17. Ribeiro DA, Marques ME, Salvadori DM. *In vitro* cytotoxic and non-genotoxic effects of gutta-percha solvents on mouse lymphoma cells by single cell gel (comet) assay. *Braz Dent J.* 2006;17(3):228-232.
18. Mosann T. Rapid colorimetric assay for growth and survival: Application to proliferation and cytotoxicity assay. *J. Immunol. Methods.* 1983;65:55-63.
19. Gangadevi, Muthumary. Preliminary studies on cytotoxic effect of fungal taxol on cancer cell lines. *African Journal of Biotechnology.* 2007;6:182-1386.
20. Rastogi L, Arunachalam J. Sunlight based irradiation strategy for rapid green

- synthesis of highly stable silver nanoparticles using aqueous garlic (*Allium sativum*) extract and their antibacterial potential. *Mat. Chem. Physics*. 2011;129: 558–563.
21. Zonooz NF, Salouti M. Extracellular biosynthesis of silver nanoparticles using cell filtrate of *Streptomyces* sp. ERI-3 *Scientia Iranica*. 2011;18(6):1631–1635.
 22. EL-Batal AI, Abd-Algawad MH, Noha MA. Gamma radiation mediated green synthesis of gold nanoparticles using fermented soybean-garlic aqueous extract and their antimicrobial activity. *Springer Plus*. 2013;2:129.
 23. El-Batal AI, Amin MA, Mona MKS, Merehan MA. Synthesis of silver nanoparticles by *Bacillus stearothermophilus* using gamma radiation and their antimicrobial activity. *World Applied Sciences Journal*. 2014;22(1):01-16.
 24. Chen P, Song L, Liu Y, Fang Y. Synthesis of silver nanoparticles by g-ray irradiation in acetic water solution containing chitosan. *Radiation Physics and Chemistry*. 2007;76:1165–1168.
 25. Kassaee MZ, Akhavana A, Sheikhb N, Beteshobabrud R. γ -Ray synthesis of starch-stabilized silver nanoparticles with antibacterial activities. *Radiation Physics and Chemistry*. 2008;77(9):1074–1078.
 26. El-Baz AF, El-Batal AI, Farag MA, Ahmed AT, Yousria MS, Shang TY. Extracellular biosynthesis of anti-*Candida* silver nanoparticles using *Monascus purpureus*. *Journal of Basic Microbiology*. 2015;55:1-10.
 27. Eha K, Sathishkumar M, Mao JK, Wak IS, Yan SY. Corynebacterium glutamicum mediated crystallization of silver ions through sorption and reduction process. *Process Biochemistry*. 2010;162:989-943.
 28. Aji DS, Basavaraja S, Deshpande R, Mahesh DB, Prabhakar BK, Venkataraman A. Extracellular biosynthesis functionalized silver nanoparticles by strain of *Cladosporium cladosporioides* fungus. *Colloids and surface B. Biointerfaces*. 2009;86:88-92.
 29. Gurunathan S, Kalishwaralal K, Vaidyanathan R, Deepak V, Ram K, Pandian S, Muniyandi J, Hariharan N, Hyun ES. Biosynthesis, purification and characterization of silver nanoparticles using *Escherichia coli*. *Colloids and Surfaces B. Biointerfaces*. 2009;74:328–335.
 30. Akhgari A, Garekani HA, Sadeghi F, Azimaian M. Statistical optimization of indomethacin pellets coated with pH-dependent methacrylic polymers for possible colonic drug delivery. *International Journal of Pharmaceutics*. 2005;305:22-30.
 31. Rastogi L, Arunachalam J. Sunlight based irradiation strategy for rapid green synthesis of highly stable silver nanoparticles using aqueous garlic (*Allium sativum*) extract and their antibacterial potential. *Mat. Chem. Physics*. 2011;129: 558– 563.
 32. Bunghez IR, Barbinta PM, Badead N, Doncea SM, Popescu BA, Ion RM. Antioxidant silver nanoparticles green synthesized using ornamental plants. *J. of Opt. and Adv. Mater*. 2012;14(11-12):1016 – 1022.
 33. Supraja S, Arumugam P. Antibacterial and anticancer activity of silver nanoparticles synthesized from cynodon dactylon leaf extract. *Journal of Academia and Industrial Research (JAIR)*. 2015;3(12).
 34. Shawkey AM, Rabeh AM, Abdullal AK, Abdellatif AO. Green nanotechnology: Anticancer activity of silver nanoparticles using *Citrullus colocynthis* aqueous extracts. *Adv. Life Sci. Technol*. 2013;13: 60-70.
 35. Vijayakumar S, Ganesan S. *In vitro* cytotoxicity assay on gold nanoparticles with different stabilizing agents. *Journal of Nanomaterials*. 2012;734398:9.
 36. Alsemari A, Alkhodairy F, Aldakan A, Al-Mohanna M, Bahoush E, Shinwari Z, Alaiya A. The selective cytotoxic anticancer properties and proteomic analysis of *Trigonella Foenum-Graecum*. *Complementary and Alternative Medicine*. 2014;1472-6882/14/114.
 37. Leclere L, Cutsem PV, Michiels C. Anticancer activities of pH- or heat-modified pectin. *Front. Pharmacol*. 2013;10:3389 - 00128.
 38. GLinsky VV, Raz A. Modified citrus pectin antimitastatic properties. *One Bullet, Multiple Targes Carbohydres*. 2009; 23444:1788-1791.

39. Irulappan MS, Barath S, Kanth M, Kalishwaralal K, Gurunathan S. Antitumor activity of silver nanoparticles in Dalton's lymphoma ascites tumor model. International Journal of Nanomedicine. 2010;5:753–762.
40. Sunita PS, Sivaraj RV, Vanathi R, Vanathi P, Rajiv P. Anticancer potential of green synthesized silver nanoparticles: Review, International Journal of Current Research. 2015;7:10.

© 2016 Ghorab et al.; This is an Open Access article distributed under the terms of the Creative Commons Attribution License (<http://creativecommons.org/licenses/by/4.0>), which permits unrestricted use, distribution and reproduction in any medium, provided the original work is properly cited.

Peer-review history:
The peer review history for this paper can be accessed here:
<http://sciencedomain.org/review-history/16264>